Preparation of Performance of Nanosilica-loaded Fluorescent Yellowing Inhibitor in Paper Made from High-yield Pulp

Mingyuan Guo,[a,b] Guanghua Zhang,[a,*] Yuqun Lu,[a] Jing Pei,[a] Lun Du,[a] Wanbin Zhang,[a] and Yongning Ma [a,*]

3-Aminopropyl-trimethoxysilane was introduced into bis-triazinyl amino-stilbene through the condensation reaction to obtain fluorescent whitening agents (FWAs) having excellent photo-stability. Tetraethoxysilane was hydrolyzed and combined with FWAs through *in situ* polymerization to obtain nanosilica-loaded yellowing inhibitors (SiO_2–FWAs). Ultraviolet (UV) spectroscopy showed that the ratios of the *trans*-isomer structure in FWAs after 3 h of UV irradiation was 5.41 times higher than those of the *cis*-isomer. Moreover, the absorption intensity in the UV region was increased distinctly after nano-silica loading. Fluorescence spectroscopy revealed that the fluorescence of SiO_2–FWAs was more intense than that of FWAs. In addition, the fluorescence quantum yield of SiO_2–FWAs reached 0.416, whereas that of the default FWAs was only 0.279. UV-aging test results showed that SiO_2–FWAs can improve the initial whiteness and anti-yellowing performance of paper made from high-yield pulp (HYP). These results indicated that the as-prepared SiO_2–FWAs not only exhibited more excellent UV absorption and fluorescence emission properties, but it also exerted better whitening and anti-yellowing effects on high-yield pulp paper than the default FWAs. The enhanced performance of SiO_2–FWAs can be ascribed to the synergy between the excellent UV-scattering effect of nanosilica and the fluorescent whitening property of FWAs.

Keywords: HYP; Yellowing inhibitor; Optical stability; Bistriazinylstilbene derivative; Nanosilica; Brightness

Contact information: a: Shaanxi Key Laboratory of Chemical Additives for Industry, Shaanxi University of Science and Technology, Xi'an 710021, China; b: College of Chemistry and Materials Science, Weinan Normal University, Wainan 714099, China;
** Corresponding authors: zhanggh@sust.edu.cn; ynma@sust.edu.cn*

INTRODUCTION

In order to solve the problems of traditional mechanical pulp such as high production costs, poor strength, low yield, large total amount of chemicals, and difficulty in post-production pollution treatment, scientists explored and invented a high-efficiency, high-quality, low-polluting pulping technology-chemical mechanical pulping in the 1970s and the resulting pulp is called high-yield pulp(HYP). The yield of HYP exceeds 65% and usually contains semi-chemical pulp (SCP), chemical mechanical pulp (CMP), wood chip groundwood pulp (RMP), thermomechanical pulp (TMP), chemical thermomechanical pulp (CTMP), stone groundwood pulp (SGW), pressed stone groundwood pulp (PGW) and other paper pulp. Among them, the alkaline peroxide mechanical pulp(APMP), established on the basis of BCTMP, introduced by ASB in the 1990s is favored by the paper industry, which yield is as high as 85% to 95%. In addition, compared with chemical pulp, high-

yield pulp has obvious characteristics of high whiteness, high strength, low fiber bundle and high printing quality, so the obtained paper products are put into the production of newsprint, coated base paper and other cultural papers. Furthermore, APMP pulping greatly simplifies the traditional pulping process, and can also save a lot of costs, which has a good development prospect. Therefore, HYP is widely used in paper industry to address the shortages of wood resource, alleviate environment deterioration, and reduce production waste (Liu *et al.* 2012; Wang *et al.* 2013; Liu *et al.* 2016; Li *et al.* 2017). However, the unseparated lignin in HYP can easily lead to yellow reversion with ambient light irradiation, and this restricts the application of HYP in high-quality paper (Cannell and Cockram 2000; Rundlöf *et al.* 2002; Manda *et al.* 2012; Vänskä *et al.* 2016). Herein, a yellowing inhibitor, used to suppress the color reversion of HYP, is an effective way to expand the usage of HYP paper (Um *et al.* 2006; Zhang *et al.* 2013; Guo *et al.* 2017).

To introduce additives having the ability to absorb ultraviolet (UV) light and/or free-radical elimination function has been reported to be one of the most effective and economical ways to suppress the color reversion of HYP, and such an approach also is relatively easy to implement industrially (Eltoni *et al.* 2006; Smt *et al.* 2013; Turkovic *et al.* 2016). One of the most used additives is fluorescent brighteners (FWAs), which are also used for pulp whitening in the paper industry and cotton industry due to the superior whitening performance and relatively low cost (Konstantinova *et al.* 1999; Hörsch *et al.* 2003; Lee *et al.* 2005; Fan *et al.* 2007; Jung and Kang 2013). Even so, the primary disadvantages of FWAs are their poor stability in long-term irradiation, low yellowing point, and sensitivity to sunlight (Konstantinova *et al.* 1999; Chen *et al.* 2014). To overcome the draw-backs of FWAs, numerous researchers have introduced fluorescent molecules to improve the photostability *via* steric hindrance in polymerization systems (Hussain *et al.* 2009; Saeed *et al.* 2014). Liu and Zhang (2011) synthesized an asymmetrical polymeric FWAs and showed that its photostability has drastically improved after polymerization. Zheng *et al.* (2016) also prepared a polymeric FWA that was based on the 4,4'-diaminostilbene-2,2'-disulfonic (DSD) acid–triazine structure, which can improve the photostability and enhance the brightness, surface strength, and smoothness of paper. Based on the above mechnism on color reversion, the most important factor is FWAs (inhibitors) that shield the UV light (convert the absorbed UV light to thermal energy). By absorbing the UV light energy before it reached the lignin, the lignin that remains in HYP not be damaged by the UV light from sunlight. Nevertheless, the use of FWAs to restrain the color reversion of HYP fails to enable long-term inhibition performance, and bare organic molecules are easily decomposed under ambient light irradiation for long durations.

Nanosilica is an excellent UV shielding agent with high reflectivity of more than 70%, superior biocompatibility, and thermal insulation properties (Medda and De 2009; Strauchs *et al.* 2012; Tang *et al.* 2012). In this paper, a nanosilica-loaded yellowing inhibitor was prepared. Here, KH-540, a silane coupling agent, was used as a bridging group to introduce FWAs into nanosilica through *in-situ* polymerization. The steric hindrance of KH-540 can improve photo stability by effectively inhibiting the photo isomerization of FWAs. Moreover, the unique UV absorption properties of nanosilica and FWAs can drastically delay the photo-aging of HYP paper.

EXPERIMENTAL

Materials

All chemicals, such as KH-540, tetraethoxysilane (TEOS), cyanuric chloride, 4,4′-diaminostilbene-2,2′-disulfonic acid (DSD acid), sodium hydroxide, absolute ethyl alcohol, acetone, and morpholine were purchased from Aladdin. All chemicals used were of industrial or analytical grade and used without further purification.

Methods

Synthesis of DSD acid–triazine fluorescent intermediate

First, DSD acid (0.0083 mol) in 5% NaOH solution (20 mL) was dropped into a solution of cyanuric chloride (0.0166 mol) in acetone (40 mL) at 0 °C to 5 °C. The pH of the system was maintained in the range 5 to 6 with NaOH (10%). The reaction mixture was stirred at 0 to 5 °C for 2 h. The temperature was then increased to between 35 and 40 °C. Morpholine (0.0166 mol) was then added, and the mixture was stirred for another 2 h. The pH of the mixture was maintained at 7 to 8. Then, KH-540 (0.0166 mol) was added to the reaction flask. The reaction mixture was heated to 80 °C for 4 h, and its pH was controlled at 9 to 10. Acetone was removed from the mixture through distillation. A precipitate was obtained after washing with acetone and filtration, and drying at 40 °C for 24 h.

The precipitate (5 g) was added to a mixture of deionized water (20 g) and anhydrous ethanol (20 g) in a three-necked flask. The reaction mixture was stirred at 60 °C for 6 h while its pH was maintained in the range 11 to 12 with NaOH (10%). After washing with anhydrous ethanol and filtration, and drying at 45 °C for 24 h, the FWAs were finally obtained. The synthetic route of FWAs is shown in Fig. 1: Yield: 82.6%, I.R. (KBr): 3378 cm^{-1} (N–H and O–H stretching); 2930, 2885 cm^{-1} (CH_2–stretching); 1618, 1572, 1505 and 1481 cm^{-1} (Ar stretching); 1356 cm^{-1} (C–N stretching); 1171 cm^{-1}(–SO_3H stretching); 1125 cm^{-1}(–CH_2–O–CH_2–stretching); and 800 cm^{-1} (Si–O stretching).

Preparation of SiO_2 and SiO_2-loaded fluorescent antiyellowing agent

Anhydrous ethanol (50 mL), deionized water (1.0 mL), TEOS (1.5 mL), and ammonia (1.7 mL) were added to a three-necked flask in accordance with a previously reported protocol for *in-situ* polymerization (Liang *et al.* 2016). The mixture was then stirred at 40 °C for 2 h. Then, aliquots of the aqueous solution containing different mass fraction of FWAs (0.10, 0.12, 0.14, 0.16, and 0.18 wt% of TEOS) were added drop-wise into the reaction system and reacted under uniform stirring at a rate of 700 rpm. Light-yellow powders were obtained after 24 h of stirring at 40 °C by removing residual FWAs and TEOS through three cycles of circulation in ethanol and drying in a vacuum oven at 40 °C for 48 h. Yield: 40.3%. I.R. (KBr): 3448 cm^{-1} (O–H stretching); 3234 cm^{-1} (N–H stretching); 2972 cm^{-1} (CH_2–stretching); 1536 cm^{-1} (Ar stretching); 1095 cm^{-1} (Si–O–Si stretching); 958 cm^{-1} (Si–OH stretching); and 800 cm^{-1} (Si–O stretching).

Nanosilica was prepared in reference to the first step of the preparation method of SiO_2–FWAs (Liang *et al.* 2016). The target product was obtained after three cycles of centrifugation/redispersion in ethanol after 12 h of reaction followed by drying in a vacuum oven at 40 °C for 48 h. Yield: 79.3%. I.R. (KBr): 3656 cm^{-1}(O–H stretching); 1095cm^{-1} (Si–O–Si stretching); 958 cm^{-1} (Si–OH stretching); and 800 cm^{-1} (Si–O stretching).

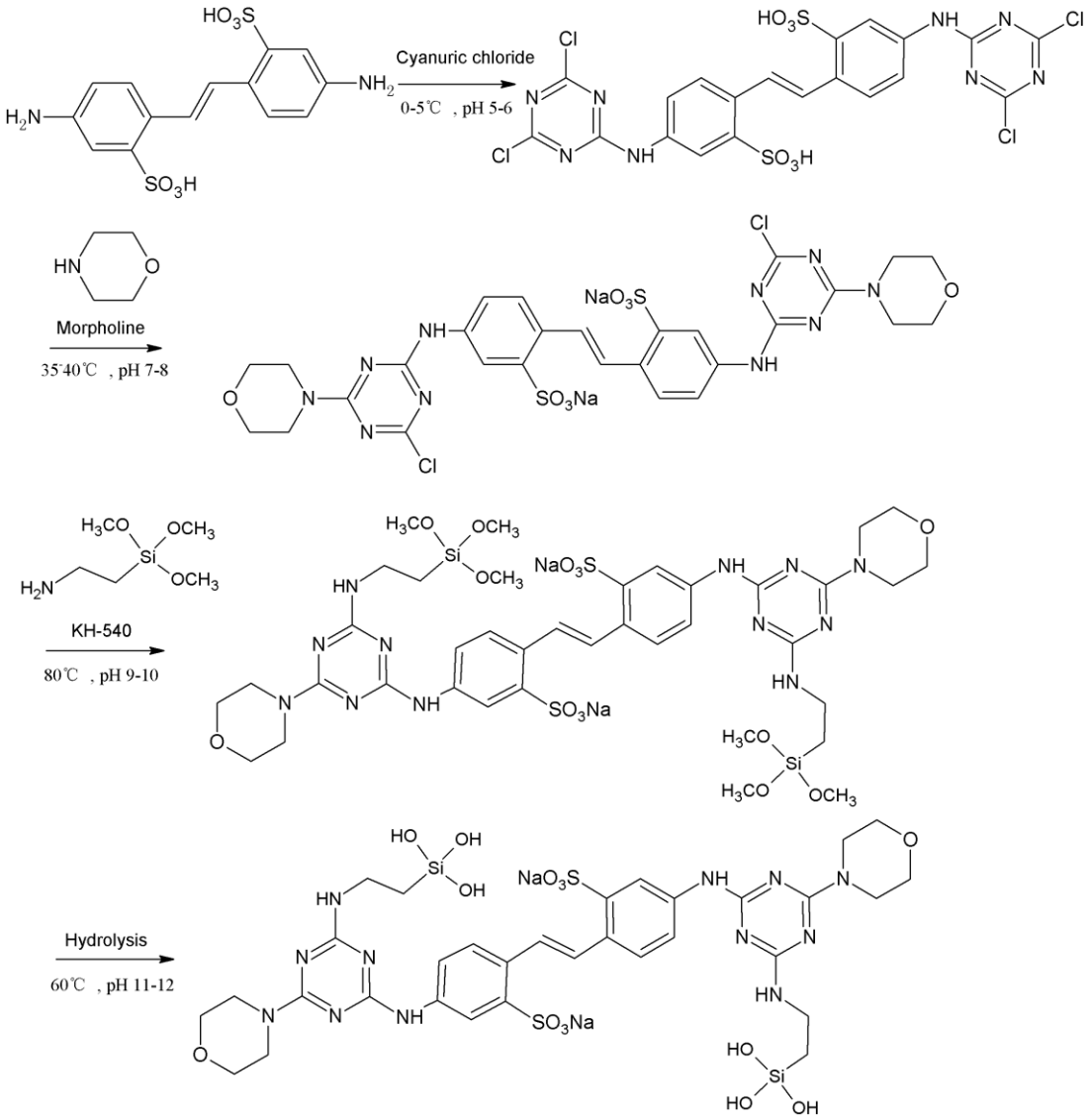

Fig. 1. Schematics of the preparation of the FWAs

Preparation of handsheets for the UV-accelerated aging test

Handsheets (100 g/m^2) for the UV-accelerated aging test were prepared in accordance with TAPPI methods (T205 SP-95) by using poplar APMPpulp (Yueyang Paper Co., Ltd, Shanghai, China) and the yield is about 88%. Surface sizing material was prepared by using 4% starch solution that had been heated at 95 °C for 30 min. Then, different contents of synthesized compounds were added. The handsheets were coated on the sizing materials by usinga coating machine (ST-1-260, Shaanxi University of Science and Technology, China). The paper samples were dried at room temperature away from light. The test method for paper brightness has been described in a previous work (Zhang *et al.* 2016).

Characterization

The structures of the prepared samples were characterized through Fourier transform infrared (FTIR, Vector-22, Bruker Corporation, Berlin, Germany) and X-ray photoelectron spectroscopy (XPS, Axis Supra, Kratos, Manchester, UK). Surface morphology was observed through transmission electron microscopy (TEM, FEI Tecnai G2 F20 S-TWIN, PEI, New York, USA). Optical performance was quantified by using an UV–visible spectrometer (UV–Vis, Cary100, Agilent, Santa Clara, USA) and fluorescent phosphorescence pyrolysis spectrometer (FluoroMax-4P, HORIBA, Tokyo, Japan). The brightness of handsheets was quantified by using a colorimeter (dominant wavelength: 425±5 nm) (ZB-A, Hangzhou Zhibang Instrument Co., Ltd., Hangzhou, China). The particle size distribution of nanocomposites was determined by a nanoparticle size surface potential analyzer (Zetasizer, NANO-ZS90, Quantachrome, Florida, USA). The UV-accelerated aging test was performed by using a ZN-100N desktop UV light resistance climate chamber (Xi'an Tongsheng Instrument Manufacturing Co. Ltd, China). The handsheets used in the experiment were prepared by using a sheet former (Shaanxi University of Science and Mechanical Equipment Factory, Xi'An, China).

RESULTS AND DISCUSSION

Structure and Morphology of SiO_2–FWAs

The XPS wide spectra (A), relative elemental contents (B), and Si2p spectra of FWAs and SiO_2–FWAs(C) are shown in Fig. 2, respectively. Figure 2A shows that both compounds contained elemental Si, and the relative Si content of SiO_2–FWAs was considerably higher than that of FWAs. The relative elemental contents of the FWAs and SiO_2–FWAs in the XPS wide spectra are shown in Fig. 2B. The C content ofSiO_2–FWAs had decreased. Nevertheless, the significant increase in the O- and Si- contents of SiO_2–FWAs compared with that in the O- and Si- contents of FWAs suggests that SiO_2–FWAs had been prepared successfully. The XPS Si2p spectra of FWAs and SiO_2–FWAs are presented in Fig. 2C, which was in agreement with the above result. As inferred from the XPS Si2p spectra of FWAs, the energies of Si–C and Si–O were 101.7 and 102.9 eV, respectively, whereas those of SiO_2–FWAs were 101.9 and 102.7 eV. The relative Si–O content of SiO_2–FWAs was higher than that of FWAs. This result illustrates that Si mainly was present in the form of SiO_2 (Si2p, 103.3 eV) in the SiO_2–FWAs.

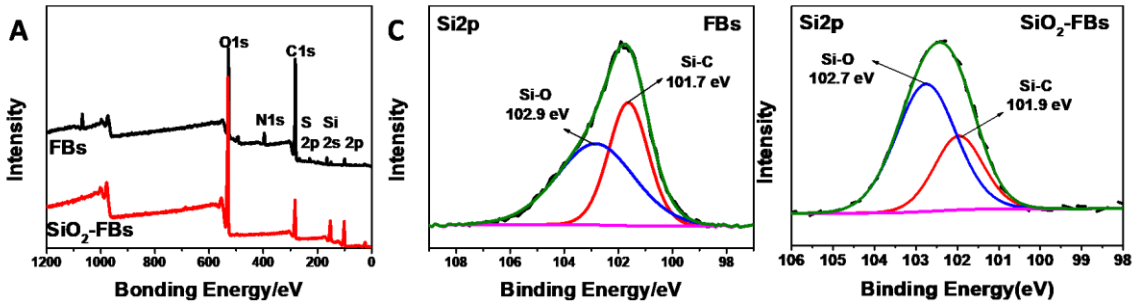

B

Compounds	Relative Content (At%)				
	C	O	Si	N	S
FWAs	70.44(284.6)	20.88(531.6)	2. 01(101.9)	4.25(398.6)	2.42(167.6)
SiO_2-FWAs	31.15(284.6)	44.78(532.6)	24.07(102.4)	-	-

Fig. 2. XPS wide spectra (A); relative elemental content in XPS wide spectra (B); and Si2p spectra (C) of FWAs and SiO_2–FWAs

Silica and SiO_2–FWAs particles were re-dispersed into ethanol for TEM and SEM imaging and particle size analysis. The results are provided in Fig. 3. The TEM images of SiO_2 (Fig. 3A) reveal that the size of pure silica particles was approximately 80±10 nm and they had a uniform size distribution. The size of the as-prepared SiO_2–FWAs had increased to 110±10 nm relative to that of SiO_2. The layer of material covering the surfaces ofSiO_2–FWAs could be attributed to the uniform cladding of FWAs on the surfaces of SiO_2 spheres. The SEM images of SiO_2 and SiO_2–FWAs (Fig. 3B) showed that numerous bumps were present on the surfaces of SiO_2–FWA particles. The surface of pure silica is smoother than that of SiO_2–FWAs. In addition, the particle size of nanosilica was approximately 50 nm to120 nm, and that of SiO_2–FWAs was approximately 80 nm to 170 nm. These results indicated that the particle size of silica had increased after modification with FWAs molecules. The above results indicated that the FWAs had successfully coated on the surfaces of nanosilica to form the SiO_2–FWAs inhibitor.

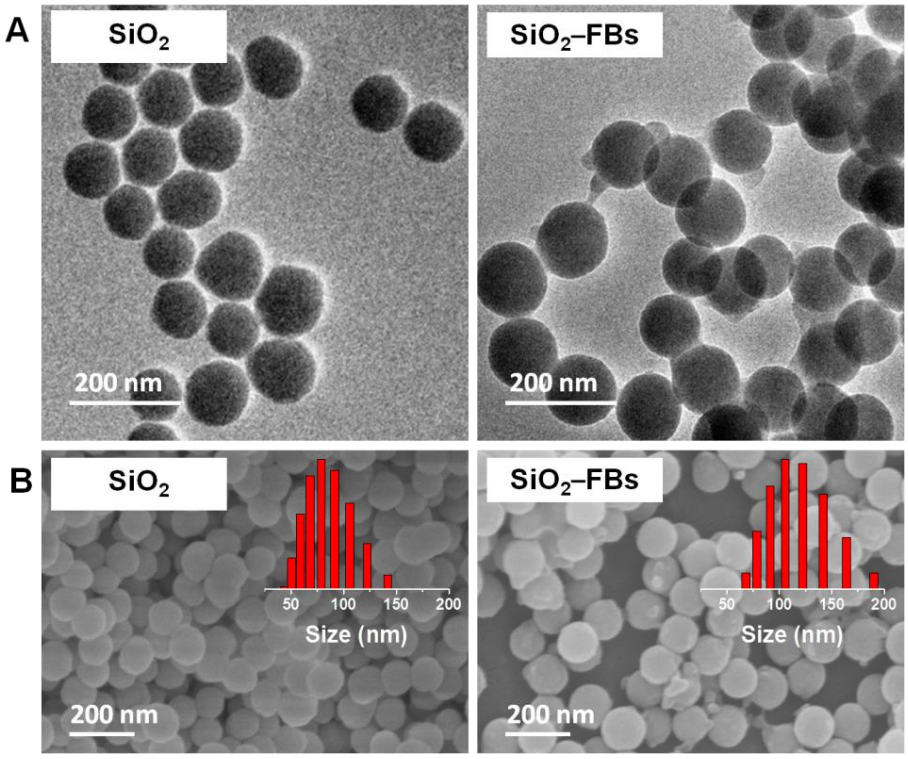

Fig. 3. TEM images (A); and SEM images and particle size distributions(B) of SiO_2 and SiO_2–FWAs

Light and thermal stability of SiO_2–FWAs

The light stability and UV absorption property of FWAs were analyzed in aqueous solution after 3 h of UV irradiation. The results are given in Fig. 4A. The two curves appeared similar, and their maximum absorption peaks were located at 348 nm. The coincidence between the absorption peaks indicated that the main structure of the prepared FWAs had not been destroyed by UV irradiation, that UV irradiation had negligible effects on the structure of FWAs. In addition, the as-prepared FWAs exhibited excellent light stability.

Light stability is an important index of the performance of the DSD acid-based FWAs. *Trans*(C_T)- and *cis*(C_c)- isomer concentrations were used as the evaluation standard. High C_T/C_C values indicated good light stability and fluorescence. The percent concentration of *cis–trans*-isomers in the solution can be expressed using a formula taken from a previous work (Liu and Zhang 2011). As shown in Fig. 4A, the C_T and C_c of FWAs after 3 h of UV light irradiation and in the absence of irradiation were 84.4% and 15.6%, respectively, and the C_T/C_C value was 5.41. These results indicated that FWAs presented good structural stability under UV irradiation. The structures of the *cis–trans*-isomers of FWAs are shown in Fig. 4B, which shows that the considerable steric hindrance exerted by the $NH–(CH_2)_2–Si(OH)_3$ group on the structure of FWAs can effectively prevent the occurrence of *cis–trans* isomerism under UV irradiation.

Figure 4C shows the UV absorption spectra of SiO_2, FWAs, and SiO_2–FWAs in aqueous solution. The blue dotted line, black solid line, and red dotted line are the absorption curves of SiO_2, FWAs, and SiO_2–FWAs, respectively. Pure SiO_2 showed excellent absorption property at wavelengths of less than 300 nm but poor performance at long wavelengths. The absorption peak in the range 250 to 400 nm is the typical peak of FWAs and was considerably stronger than that of pure SiO_2. Compared with that of pure

samples, the intensity of SiO_2–FWAs in the whole UV region was increased. The absorption region had expanded to approximately 500 nm. The improvement in absorption property may be caused by the strong absorption induced by the interaction between SiO_2 and FWAs and is beneficial for UV light absorption and attenuating paper reversion. Therefore, the good UV-shielding property of the as-prepared SiO_2–FWAs confers the superior color-inhibiting property of SiO_2–FWAs over that of pure FWAs.

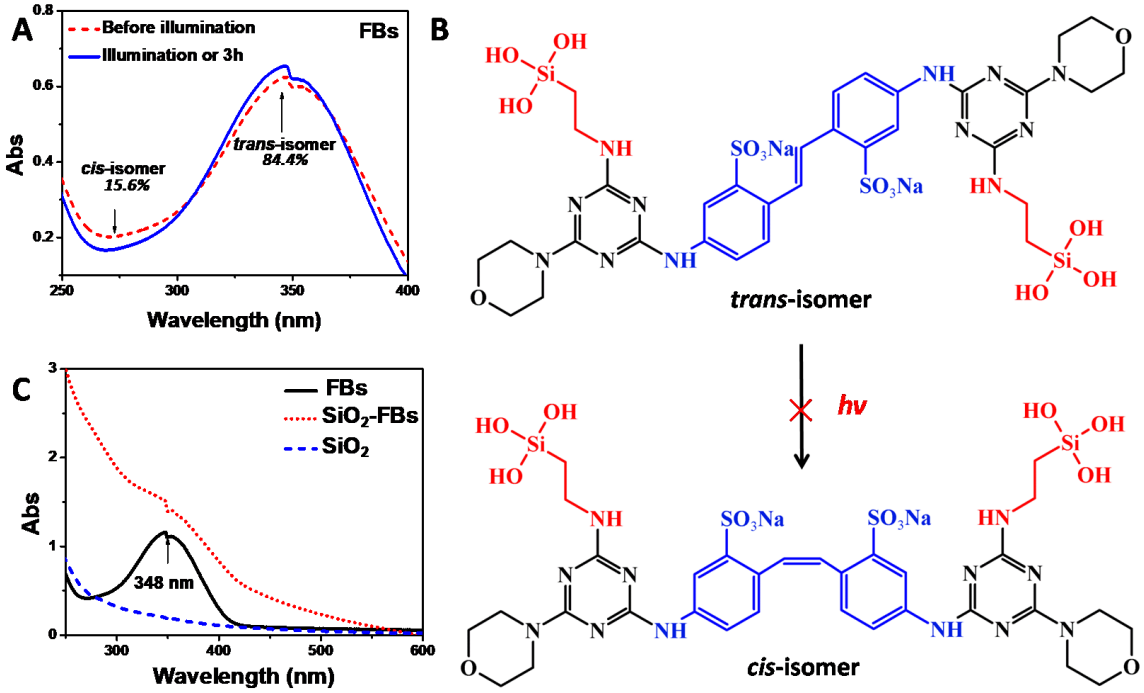

Fig. 4. Light stabilities of FWAs in aqueous solution(A);*cis*–*trans*-isomerism of FWAs(B); and UV absorption spectra of FWAs, SiO_2–FWAs, and SiO_2(C)

Fluorescence spectra of FWAs and SiO_2–FWAs

Fluorescent brightness additives primarily enhance the whiteness and brightness of textiles and papers by increasing UV-blocking properties through absorbing light in the near-UV region and re-emitting light at long wavelengths in the blue and visible regions. The fluorescence spectra of FWAs and SiO_2–FWAs are shown in Fig. 5A. The FWAs and SiO_2–FWAs can absorb UV light at 355 nm and 357 nm (λ_A), respectively, and re-emit light at 435 nm and 434 nm (λ_F) in the blue region, respectively. In addition, the fluorescence intensity of SiO_2–FWAs was stronger than that of FWAs. This result indicates that the fluorescence emission performance and conversion rate of UV light absorbed by the as-prepared SiO_2–FWAs were higher than those of FWAs. The maximum emission wavelength was almost unchanged and can complement the yellow color of paper for white light emission. Thus, the whiteness of the modified paper persists under ambient or UV light irradiation.

The Stokes shift ($\Delta\sigma$) is a parameter that indicates the difference between the properties and structure of the fluorophores in the ground state S_0 and the first excited state S_1. Large $\Delta\sigma$ values represent high energy losses in electron transition. The $\Delta\sigma$ values (cm^{-1}) were calculated by using Eq (1),

$$\Delta\sigma = \frac{(\lambda_F - \lambda_A)\times 10^7}{\lambda_F \lambda_A} \quad (1)$$

The SiO_2–FWAs were more photo stable than FWAs (Wei *et al.* 2004; Magalhães *et al.* 2006), as indicated by the considerably higher $\Delta\sigma$ values of FWAs ($\Delta\sigma$ = 5180.5 cm^{-1}) than those of SiO_2–FWAs ($\Delta\sigma$ = 4969.7 cm^{-1}) (Fig.5A).

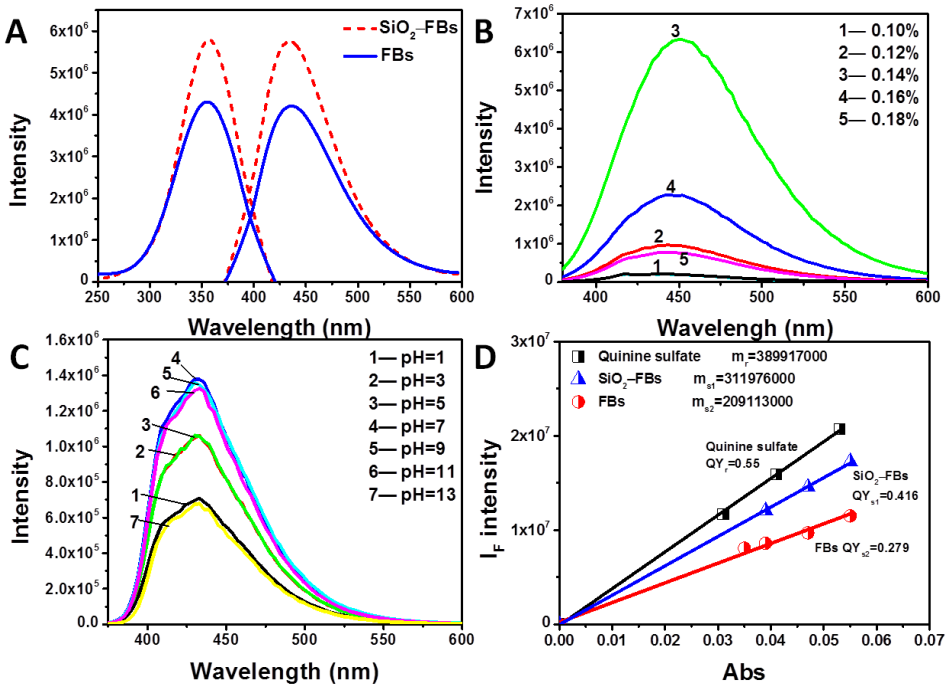

Fig. 5. Fluorescence spectra of FWAs and SiO_2–FWAs in aqueous solution with the same concentration (A); Changes in the fluorescence emission intensity of SiO_2–FWAs with the changes in the added content of FWAs (B) (0.10, 0.12, 0.14, 0.16, and 0.18 wt%) and pH values (C); and fluorescence quantum yield of FWAs and SiO_2–FWAs in aqueous solution (D).

Figure 5B provides the fluorescence emission spectra of SiO_2–FWAs synthesized with various FWAs contents (0.10, 0.12, 0.14, 0.16, and 0.18 wt%). The fluorescence intensity of SiO_2–FWAs first increased and then decreased as the FWAs loading content was increased. The optimal FWAs content was 0.14wt% given that it provided the maximum fluorescence intensity of I_F= 6.36×10^6. This result indicates that the most suitable fluorescent concentration was approximately 0.14 wt%. The fluorescence spectra of SiO_2–FWAs in aqueous solutions with different pH values are displayed in Fig. 5C. Fluorescence intensity first increased and then decreased as the solution pH was increased. The maximum fluorescence emission intensity corresponded to pH=7. Thus, the SiO_2–FWAs can be used in neutral-to-alkaline environments. The value of fluorescence quantum yield (*QY*) directly reflects the whitening ability of fluorescent whitener. The calculation method of *QY* is shown in Eq. (2), and the quinine sulfate (QY_r= 0.55) was used as reference substance. The *QY* value of SiO_2–FWAs (Fig.5D) was 0.416, which was higher than that of the default FWA (0.279). This result indicates that the fluorescence emission ability of SiO_2–FWAs was better.

$$QY_S = QY_r \left(\frac{m_S}{m_r}\right)\left(\frac{n_S}{n_r}\right)^2 \quad (2)$$

In Eq. 2, QY_s and QY_r represent the fluorescence quantum yields of the sample and quinine sulfate, respectively. The m_s and m_r denote the slope of the fitted line of integrated fluorescence intensity and the corresponding absorbance of the sample, respectively. The n_s and n_r are the refractive index of the solution of the sample (water, 1.325) and quinine sulfate (0.1mol/L sulfuric acid, 1.369), respectively.

SEM images of SiO_2–FWAs applied to paper surfaces

The SiO_2–FWAs were dispersed into starch solution at a mass fraction of 1.0% and coated on the surfaces of handsheets. The surface morphology of the handsheets was then investigated. The results for the blank sample (A) and sample treated with SiO_2–FWAs (B) are shown in Fig. 6. The large number of filiform fibers (red dotted circle) on the surfaces of blank handsheets (Fig. 6A) resulted from fiber tearing and oxidation during processing. These filamentous fibers easily undergo reversion upon exposure to UV light. Reversion is the primary reason for the yellowing of HYP paper. As illustrated in Fig. 6B, the surfaces of paper fibers become covered with a layer of SiO_2–FWAs nanospheres upon treatment with SiO_2–FWAs. The as-prepared SiO_2–FWAs can prevent light from irradiating the surface of paper directly and suppresses paper aging. Moreover, SiO_2–FWAs can improve initial paper brightness by converting absorbed UV light to blue fluorescent light, which complements yellow light to enable white light emission. The above analysis shows that SiO_2–FWAs is an excellent inhibitor for preventing yellowing of HYP paper. It exhibits UV-shielding properties and fluorescent whitening performance.

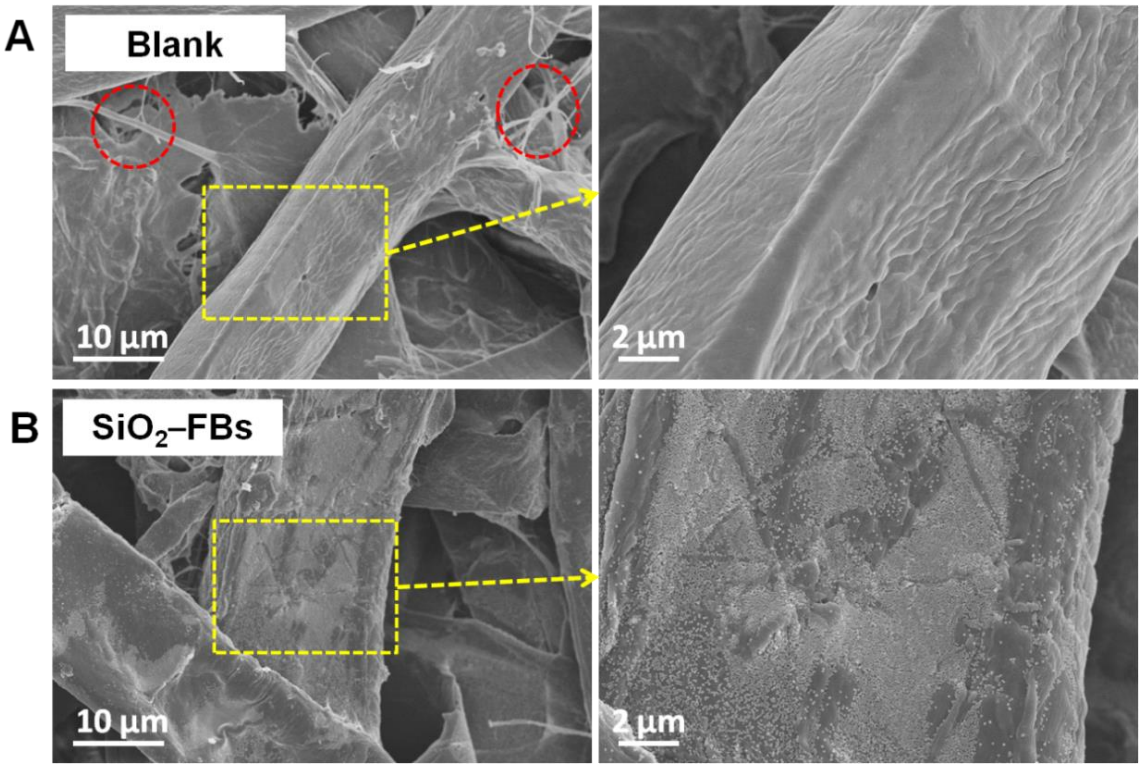

Fig. 6. SEM images of blank paper (A) and paper treated with SiO_2–FWAs (B)

Changes in the surface brightness of paper sheets under UV irradiation

Brightness and yellowing value (PC values) are important parameters for evaluating the antiyellowing performance of paper. Therefore, the brightness of handsheets coated with SiO_2–FWAs and FWAs was quantified, and PC values were calculated in reference to a previous work (Liu *et al.* 2015). The PC values of sheets coated with SiO_2–FWAs and FWAs were compared with those of blank paper sheets.

The SiO_2–FWAs were added at different concentrations (0.0, 0.2, 0.4, 0.6, 0.8, 1.0, 1.2, and 1.4 wt%) to starch solutions and coated on handsheets surface to prepare samples for the evaluation of antiyellowing performance. The samples were dried at room temperature, and their brightness was tested. The results are shown in Fig. 7A. The initial brightness of handsheets treated with SiO_2–FWAs was higher than that of blank paper. The brightness of the tested paper coated with 0.2 wt% SiO_2–FWAs had increased from 75.5 ISO% (blank paper) to 77.1 ISO%. In addition, the brightness of the paper sheets first increased with increasing concentration, and the whiteness value of the paper coated with 1.0 wt% SiO_2–FWAs was 79.4 ISO%, which is higher than that of the blank paper (a difference of 3.9 ISO%). The gradual reduction in the brightness of the paper with the further increase in coating concentration was attributed to the fluorescence quenching of SiO_2–FWAs. The above analysis indicates that the optimal coating concentration of SiO_2–FWAs was 1.0 wt%.

The changes in the brightness and PC values of coated and uncoated paper sheets after irradiation are shown in Figs.7B and 7C. The handsheets treated with SiO_2–FWAs exhibited the highest brightness value of 79.2 ISO%, which was higher than that of blank (change by 2.7%) and FWAs-coated sheets (0.94%). After 38 h of aging, the brightness of blank paper, FWAs-coated, and SiO_2–FWAs-coated sheets were decreased to 59.9 ISO%, 66.3 ISO%, and 68.5 ISO%, respectively, with relative eduction rates of 16.6%, 11.9%, and 10.7%, respectively. These results indicated that the ability of SiO_2–FWAs to increase brightness and inhibit aging was superior to that of FWAs and demonstrated that nanosilica can effectively improve the paper-brightening performance of FWAs. Figure7C shows that the SiO_2–FWAs-coated paper had the lowest PC value, followed by FWAs-coated paper. The blank paper sheets exhibited the highest PC value. Therefore, SiO_2–FWAs demonstrate good antiyellowing performance.

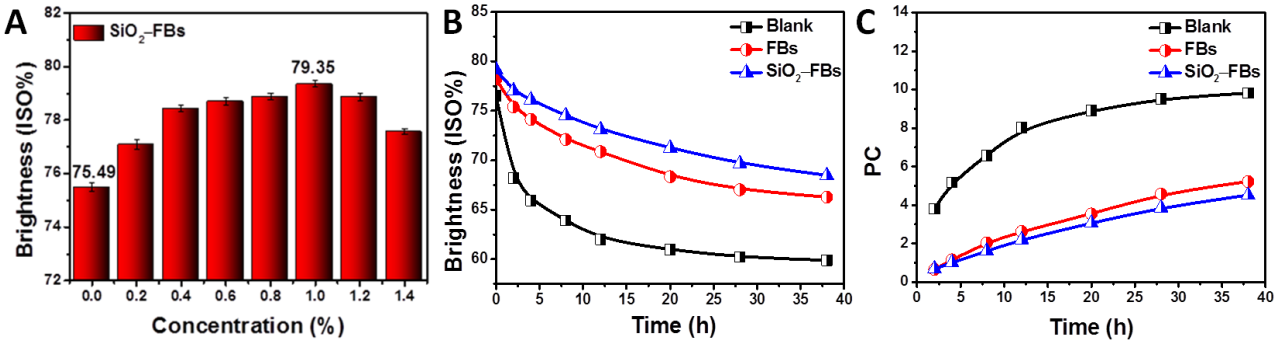

Fig. 7. Brightness of paper treated with different concentrations of SiO_2–FWAs(A) (Coating weights of the starch solution was 0.4 g/m^2, and the SiO_2–FWAs contents were 0.0, 0.2, 0.4, 0.6, 0.8, 1.0, 1.2 and 1.4 wt%, and the FWAs in SiO2–FWAs was 0.14% wt% TEOS). Changes in the brightness (B); and PC (C) of paper sheets as a function of UV irradiation time (SiO_2–FWA content was1.0 wt%).

Antiyellowing mechanism of action in HYP paper

The brightness and tristimulus values of paper sheets aged for different durations were measured by using a whiteness meter, and the corresponding chromaticity coordinates were then calculated (Table 1). The trend shown by the yellowing of sheets under ultraviolet light is described by the 1931-CIE chromaticity coordinates (as shown in Fig.8). In the 1931-CIE image, point *a* (0.3561, 0.3450) and point *b* (0.3669, 0.3511) are the color coordinates of the paper sheets before and after 16 h of UV aging, respectively. The gradual movement of the color coordinate of the paper sample away from the white light point *c* (0.3300, 0.3300) to the yellow light area during UV aging indicates that the paper sample had undergone yellowing. The chromaticity coordinate of SiO_2–FWAs (0.1574, 0.1078) was obtained by importing its fluorescence emission spectral data into CIE software and is shown in the 1931-CIE image. It is located in the blue region. The straight line drawn through points *s* and *c* shows that the chromaticity coordinate points *a* and *b* of the paper are located near the extension cord of line *c*–*s*. This result shows that SiO_2–FWAs exerted a good physical whitening effect on the paper sample.

Table 1. Brightness and Relevant Parameters of Paper Sheets at Different Light Irradiation Times

Aging Time (h)	Brightness	Tristimulus Values			Chromaticity	Coordinates
	(ISO%)	*X*	*Y*	*Z*	*X′*	*Y′*
0	69.75	82.53	79.95	69.26	0.3561	0.3450
2	67.28	81.66	78.89	66.89	0.3590	0.3469
4	66.07	81.30	78.29	65.66	0.3609	0.3476
8	64.16	80.38	77.28	63.68	0.3632	0.3491
12	62.67	79.60	76.41	62.15	0.3649	0.3502
16	61.46	79.25	75.84	60.93	0.3669	0.3511

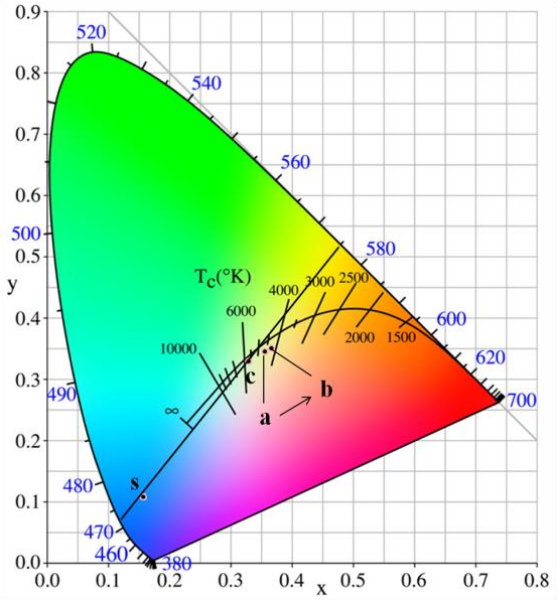

Fig. 8. 1931-CIE image of paper yellowing and color coordinate of SiO_2–FWAs.

The antiyellowing mechanism was inferred on the basis of the above results and is illustrated in Fig. 9. Three reactions occur in the SiO_2–FWA-coated paper upon UV irradiation. First, most of the ultraviolet light is absorbed, converted into other forms of energy, and then released to the atmosphere. Second, the FWAs molecules loaded on the surfaces of silica nanospheres absorb UV light and emit blue-violet fluorescence with a wavelength of 420 nm to 480 nm. Finally, the destruction of lignin molecules under direct UV irradiation results in the degradation of lignin and the development of yellow coloration. Furthermore, the blue-violet light emitted by fluorescent molecules complements the yellow light emitted by paper. This complementation results in white light emission. The mechanism for suppressing paper yellowing of as-prepared SiO_2–FWAs can be summarized as follows:

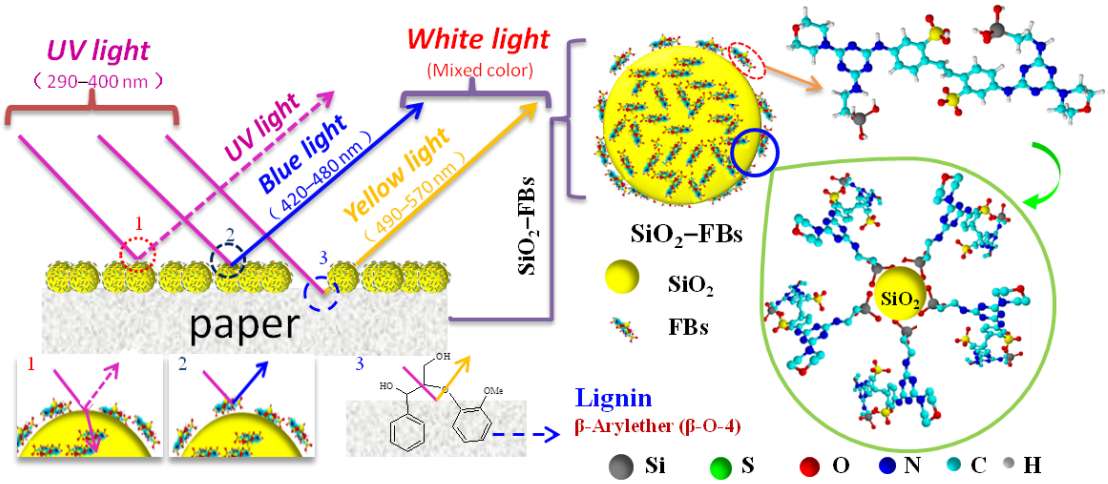

Fig. 9. Yellowing inhibition mechanism of SiO_2–FWA

CONCLUSIONS

1. The nanosilica-loaded antiyellowing agent SiO_2–FWA was successfully prepared by introducing fluorescent whitening agents (FWAs) with silicon hydroxyls on the surfaces of nanosilica particles through *in-situ* polymerization.
2. Optical performance test results indicated that the UV absorption and fluorescence emission performance of the as-prepared SiO_2–FWAs were superior to those of pure FWAs.
3. The remarkable whitening and antiyellowing properties of SiO_2–FWAs could be attributed to the synergy between silica and FWAs.

ACKNOWLEDGMENTS

This study was supported by the National Natural Science Foundation of China (31670596), Key Laboratory Scientific Research Program Project of the Education Department of Shaanxi Provincial Government (20JS048), and Scientific Research Program Project of Weinan Normal University (20RC+9).

REFERENCES CITED

Cannell, E., and Cockram, R.(2000). "The future of BCTMP," *Pulp Paper* 74, 61, 63, 65-66, 68-70, 72, 74-76.

Chen, R., Qu, J., Zhao, Q., and He, J.(2014). "Environmental impact on the light and perspiration stability of triazinylstilbene fluorescent brighteners on cotton fabrics," *Fibers Polymers* 15(9), 1915-1920. DOI: 10.1007/s12221-014-1915-z

Eltoni, A. M., Yin, S., and Sato, T. (2006). "Silica coating and photochemical properties of layered double hydroxide/4,4'-diaminostilbene-2,2'-disulfonic acid nanocomposite," *J. Colloid Interface Sci.* 293(2), 449-454. DOI: 10.1016/j.jcis.2005.06.057

Fan, X., Zhang, F., Zhang, G., and Li, G. (2007). "Kinetics and mechanism study on the preparation of 4,4′-diaminostilbene-2,2′-disulfonic acid by reduction of 4,4′-dinitrostilbene-2,2′-disulfonic acid with zero-valent iron," *Dyes Pigments* 75(2), 373-377. DOI: 10.1016/j.dyepig.2006.06.014

Guo, M. Y., Zhang, G. H., Du, L., Zheng, H., and Liu, G. J. (2017). "Water-soluble, antiyellowing polymeric fluorescence brighteners," *J. Appl. Polym. Sci.*134, 45536. DOI: 10.1002/app.45536

Hörsch, P., Speck, A., and Frimmel, F. H. (2003). "Combined advanced oxidation and biodegradation of industrial effluents from the production of stilbene-based fluorescent whitening agents," *Water Research* 37(11), 2748-2756. DOI: 10.1016/s0043-1354(03)00061-7

Hussain, M., Khan, K.M., Ali, S.I., Parveen, R., and Shim, W. S. (2009). "Synthesis and properties of symmetrically substituted 4,4′-bis(1,3,5-triazinyl)-diamino stilbene-2,2′-disulfonic acid derivatives as UV absorbing and fluorescent whitening agents," *Fibers Polymers* 10(4), 407-412. DOI: 10.1007/s12221-009-0407-z

Jung, J., and Kang, Y. (2013). "The synthesis and properties of asymmetrically substituted 4,4'-bis(1,3,5-triazine-6-yl)diaminostilbene-2,2'-disulfonic acid derivatives as fluorescent brighteners [II]," *B. Korean Chem. Soc.* 34, 2131-2137. DOI: 10.5012/bkcs.2013.34.7.2131

Konstantinova, T. N., Konstantinov, H. I., and Betcheva, R. I. (1999). "The synthesis and properties of some unsaturated triazinylstilbene fluorescent brightening agents," *Dyes Pigments* 43(3), 197-201.DOI: 10.1016/S0143-7208(99)00061-3

Lee, J. K., Um, S., Kang, Y., and Baek, D. (2005). "The synthesis and properties of asymmetrically substituted 4,4'-bis(1,3,5-triazin-6-yl)diaminostilbene-2,2'-disulfonic acid derivatives as fluorescent brighteners," *Dyes Pigments* 64(1), 25-30. DOI: 10.1016/j.dyepig.2004.03.016

Li, H., Zhang, H., Legere, S., Ni, Y., Qian, X., Cheng, H., Zhang, F., and Li, X. (2017). "Estimating the inter-fiber bonding capacities of high-yield pulp (HYP) fibers by analyzing the fiber surface lignin and surface charge," *BioResources* 13(1), 1122-1131. DOI: 10.15376/biores.13.1. 1122-1131

Liang, J., Wang, L., Bao, J., and He, L. (2016). "SiO_2-g-PS/fluoroalkylsilane composites for superhydrophobic and highly oleophobic coatings," *Colloid Surface A* 507, 26-35. DOI: 10.1016/j.colsurfa.2016.07.056

Liu, G. J., Zhang, G. H., Wang, P., Xiang, R., and Fu, X. L. (2015). "Synthesis and application of polymeric fluorescent compounds based on coumarin," *BioResources* 10(3), 4784-4794. DOI: 10.15376/biores.10.3.4784-4794

Liu, H., Chen, Y., Zhang, H., Yuan, Z., Zou, X., Zhou, Y., and Ni, Y. (2012). "Increasing

the use of high-yield pulp in coated high-quality wood-free papers, from laboratory demonstration to mill trials," *Ind. Eng. Chem. Res.* 51(11), 4240-4246. DOI: 10.1021/ie2029514

Liu, J., and Zhang, G. H. (2011). "The synthesis and study on optical characteristics of the asymmetrical polymerizable fluorescent brighteners," *Inter. J. Polymer. Mater. Polymer. Biomater* 60 (2), 199-211. DOI: 10.1080/00914037.2010.504170

Liu, Y. Y., Liu, M. R., Li, H. L., Li, B. Y., and Zhang, C. H. (2016). "Characteristics of high yield pulp fibers by xylanase treatment," *Cellulose* 23(5), 1-9. DOI: 10.1007/s10570-016-1032-9

Manda, B. M., Blok, K., and Patel, M. K. (2012). "Innovations in papermaking, an LCA of printing and writing paper from conventional and high yield pulp," *Sci. Total Environ.* 439(1), 307-320. DOI: 10.1016/j.scitotenv.2012.09.022

Medda, S. K., and De, G. (2009). "Inorganic-organic nanocomposite based hard coatings on plastics using in situ generated nano-SiO_2 bonded with ≡Si-O-Si-PEO hybrid network," *Ind. Eng. Chem. Res.* 48(14), 4326-4333. DOI: 10.1021/ie801632k

Rundlöf, M., Eriksson, M., Ström, H., and Wågberg, L. (2002). "Effect of mannanase and lipase on the properties of colloidal wood extractives and their interaction with mechanical pulp fines," *Cellulose* 9(2), 127-137. DOI: 10.1023/a:1020143825530

Saeed, A., Shabir, G., and Batool, I. (2014). "Novel stilbene-triazine symmetrical optical brighteners, synthesis and applications," *J. Fluoresc.* 24(4), 1119-1127. DOI: 10.1007/s10895-014-1392-1

Smt, G., Razavi, S. H., and Mousavi, S. M. (2013). "Comparison of antioxidant and free radical scavenging activities of biocolorant synthesized by *Dietzia natronolimnaea* HS-1 cells grown in batch, fed-batch and continuous cultures," *Ind. Crop Prod.* 49(49), 10-16. DOI: 10.1016/j.indcrop.2013.03.019

Strauchs, A., Mashkin, A., and Schnettler, A .(2012). "Effects of SiO_2 nanofiller on the properties of epoxy resin based syntactic foam," *IEEE T. Dielect. El. In.* 19(2), 400-407. DOI: 10.1109/tdei.2012.6180231

Tang, J., Chen, Y. F., Liu, H. L., Huo, Y. L., and Wang, C. P. (2012). "Preparation and microstructures of nano-porous SiO_2thermal insulation materials by freeze-casting of SiO_2 in TBA/H_2O suspensions," *Key Engineer. Mater.* 512-515, 315-318. DOI: 10.4028/www.scientific.net/KEM.512-515.315

Turkovic, V., Engmann, S., Tsierkezos, N., Hoppe, H., Madsen, M., Rubahn, H. G., Ritter, U., and Gobsch, G. (2016). "Long-term stabilization of organic solar cells using UV absorbers," *ACS Appl. Mater. Inter.* 49(12), 125604. DOI: 10.1088/0022-3727/49/12/125604

Um, S. I., Lee, J. K., Kang, Y., and Baek, D. J. (2006). "The synthesis and properties of triazine–stilbene fluorescent brighteners containing the phenolic antioxidant [II]," *Dyes Pigments* 70(2), 84-90. DOI: 10.1016/j.dyepig.2005.04.005

Vänskä, E., Vihelä, T., Peresin, M. S., Vartiainen, J., Hummel, M., and Vuorinen, T. (2016). "Residual lignin inhibits thermal degradation of cellulosic fiber sheets," *Cellulose* 23(1), 199-212. DOI: 10.1007/s10570-015-0791-z

Wang, W., Yang, G. H., and Chen, J. C. (2013). "Effect of xylanase treatment on papermaking properties of poplar high yield pulp," *Adv. Mater. Res.* 690-693(01), 1322-1326. DOI: 10.4028/www.scientific.net/AMR.690-693.1322

Zhang, G., Hua, Z., Guo, M., Lun, D., Liu, G., and Peng, W. (2016). "Synthesis of polymeric fluorescent brightener based on coumarin and its performances on paper as light stabilizer, fluorescent brightener and surface sizing agent," *Appl. Surf. Sci*. 367,

167-173. DOI: 10.1016/j.apsusc.2016.01.110
Zhang, H., Lei, M., Du, F., Li, H., and Wang, J. (2013). "Using an optical brightening agent to boost peroxide bleaching of a spruce thermomechanical pulp," *Ind.Eng. Chem. Res.* 52(36), 13192-13197. DOI: 10.1021/ie401645r

Article submitted: May 30, 2020; Peer review completed: July 19, 2020; Revised version received and accepted: August 6, 2020; Published: October 9, 2020.
DOI: 10.15376/biores.15.4.8784-8799